J Mater Sci: Mater Med (2010) 21:1463–1471
DOI 10.1007/s10856-010-4025-5

Effect of MgO contents on the mechanical properties and biological performances of bioceramics in the MgO–CaO–SiO_2 system

Xianchun Chen · Jun Ou · Yan Wei · Zhongbing Huang · Yunqing Kang · Guangfu Yin

Received: 7 August 2009 / Accepted: 1 February 2010 / Published online: 17 February 2010

Abstract The aim of this research was to investigate the effect of the chemical composition on the mechanical properties, bioactivity, and cytocompatibility in vitro of bioceramics in the MgO–CaO–SiO_2 system. Three single-phase ceramics (merwinite, akermanite and monticellite ceramics) with different MgO contents were fabricated. The mechanical properties were tested by an electronic universal machine, while the bioactivity in vitro of the ceramics was detected by investigating the bone-like apatite-formation ability in simulated body fluid (SBF), and the cytocompatibility was evaluated through osteoblast proliferation and adhesion assay. The results showed that their mechanical properties were improved from merwinite to akermanite and monticellite ceramics with the increase of MgO contents, whereas the apatite-formation ability in SBF and cell proliferation decreased. Furthermore, osteoblasts could adhere, spread and proliferate on these ceramic wafers. Finally, the elongated appearance and minor filopodia of cells on merwinite ceramic were more obvious than the other two ceramics.

1 Introduction

Since Hench et al. [1] discovered a group of special glasses based on the 45S5 bioglass, other glasses and glass–ceramics differing in chemical composition and properties have been developed for biomedical applications [2–6]. Previous studies showed that bioglasses and glass–ceramics containing CaO and SiO_2 could induce apatite formation in simulated body fluid (SBF) [4, 7], and extensive investigations confirmed that wollastonite ($CaSiO_3$) ceramics presented good osteoconduction and could directly bond to the bone in vivo [8–10]. Although wollastonite ceramics possessed good bioactivity, the mechanical strength was too low [10].

Consequently, Nakajima et al. developed Mg-containing CaO–SiO_2 based diopside ($CaMgSi_2O_6$) ceramics to be used as biomaterials, and found that diopside exhibited apatite-formation ability in SBF and could closely bond to the bone tissue when being implanted in rabbits [11–13]. In addition to further in vitro and in vivo studies, Nonami et al. [14] also tested the mechanical property of the diopside ceramics and found the significant improvement in mechanical property compared with $CaSiO_3$ and hydroxyapatite (HA) ceramics. Chang et al. investigated akermanite ($Ca_2MgSi_2O_7$) and bredigite ($Ca_7MgSi_4O_{16}$) ceramics in the MgO–CaO–SiO_2 system, and the results suggested that they showed good bioactivity and mechanical properties. Moreover, the ionic products from the ceramics could stimulate cell proliferation [15–17]. Recently, a series of studies on monticellite ($CaMgSiO_4$) and merwinite ($Ca_3MgSi_2O_8$) ceramics have been carried out in our lab, and the results revealed that monticellite and merwinite ceramics exhibited biological performances and mechanical properties similar to akermanite and bredigite ceramics [18, 19]. All the above results showed that the contents of Mg might be the key factor affecting the mechanical properties of CaO–SiO_2 based ceramics.

It is well known that Mg inhibited phase transformation from amorphous calcium phosphate to HA in SBF and the growth rate of HA diminished quickly with an increase of Mg content in glass [20]. Furthermore, some documents also reported that Mg ions could significantly enhance osteoblast

X. Chen · J. Ou · Y. Wei · Z. Huang · Y. Kang · G. Yin (✉)
College of Materials Science and Engineering, Sichuan University, Chengdu 610064, Sichuan, People's Republic of China
e-mail: nic0700@scu.edu.cn

adhesion [21] and directly stimulate osteoblast proliferation [22]. These days, Ni et al. developed three composite bioceramics (MgO wt% = 8.59, 14.32 and 20.05; Mg/Ca molar ratio = 0.71, 1.65 and 3.85, respectively) in the $MgO–CaO–SiO_2$ system, and they found that Mg might play an important role in affecting the mechanical and biological properties of $CaO–SiO_2$ based composite ceramics [23]. However, the present data are still scarce, and more work needs to be done for confirming the above role of Mg and the appropriate Mg contents in composite or single-phase ceramics in the $MgO–CaO–SiO_2$ system.

Therefore, the aim of this study was to compare the properties of three single-phase ceramics (merwinite, akermanite, and monticellite ceramics) with different MgO contents (Mg/Ca mol ratios = 0.33, 0.5 and 1, respectively) and to investigate the potential relationship between the chemical composition and the properties (i.e., mechanical and biological properties) of bioceramics in the $MgO–CaO–SiO_2$ system.

2 Materials and methods

2.1 Preparation of the ceramics

First of all, three kinds of ceramic powders with different MgO contents were synthesized. Akermanite ($Ca_2MgSi_2O_7$, MgO wt% = 14.78, Mg/Ca molar ratios = 0.5) powders were synthesized by sol–gel process using tetraethyl orthosilicate ($(C_2H_5O)_4Si$, TEOS), magnesium nitrate hexahydrate ($Mg(NO_3)_2{\cdot}6H_2O$) and calcium nitrate tetrahydrate ($Ca(NO_3)_2{\cdot}4H_2O$) as raw materials and HNO_3 as a precipitant according to Chengtie Wu [16]. Then, Monticellite ($CaMgSiO_4$, MgO wt% = 25.76, Mg/Ca molar ratios = 1) and merwinite ($Ca_3MgSi_2O_8$, MgO wt% = 12.26, Mg/Ca mol ratios = 0.33) powders were prepared by the same process and raw materials [18, 19]. Three single-phase ceramic wafers of monticellite, akermanite and merwinite were prepared by uniaxial pressing of the corresponding powders under 20 MPa and sintering the compacts at 1480, 1350 and 1400°C for 6 h, respectively, followed by slow furnace cooling. The nominal chemical composition of there ceramics is listed in Table 1.

Table 1 The nominal chemical composition of three ceramics

Ceramics	Mg/Ca molar ratios	Composition (wt%)		
		MgO	CaO	SiO_2
Monticellite ($CaMgSiO_4$)	1	25.76	35.84	38.40
Akermanite ($Ca_2MgSi_2O_7$)	0.5	14.78	41.14	44.08
Merwinite ($Ca_3MgSi_2O_8$)	0.33	12.26	51.18	36.56

The 3-point bending strength and Young's modulus of three ceramics were measured at a crosshead speed of 0.5 mm/min with span length of 30 mm following the national standard GB/T 6569-2006. The fracture toughness was evaluated at room temperature through the single edge notched precracked beam (SEPB) method according to the national standard GB/T 23806-2009. For the evaluation of the bioactivity and cytocompatibility in vitro of the above ceramics, the wafers with dimension of $\Phi 10 \times 2.0$ mm^2 were prepared and sterilized at 121°C for 30 min. Before the mechanical and biological tests, all ceramic wafers were polished using 0.5 mm diamond paste.

The sintered ceramics were identified by X-ray diffraction (XRD; X'Pert MPD 3 kW, Philips, Eindhoven, The Netherlands) with a step size of 0.02° in the 2θ range of 15–70°. The mechanical properties were evaluated by an electronic universal machine (AG-10TA, Shimadzu, Kyoto, Japan) under the same conditions. The Archimedes' technique was used to measure the apparent densities of three ceramics in distilled water at room temperature, and the relative densities were calculated from the apparent and true densities [18].

2.2 Apatite-formation ability of the ceramics in SBF

Three kinds of single-phase ceramic wafers were soaked in SBF solution (pH value = 7.40) at 37°C for 14 days, respectively, and the ratio of wafer surface area to solution volume of SBF was 0.1 cm^2/ml. The SBF solution was prepared according to the process described by Kokubo [24].

After the prescribed soaking time, these ceramic wafers were taken out, rinsed three times with double-distilled water, and dried for 24 h at room temperature. Then they were characterized by XRD with a step size of 0.02° in the 2θ range of 20–70° and scanning electron microscopy (SEM, JSM-5900LV, Hitachi, Tokyo, Japan). Bone-like apatite formation on ceramic surfaces was determined by fourier transform infrared spectroscopy (FTIR, Spectrum One, PerkinElmer, Jersey, New Jersey, USA). The changes in P ion concentrations in SBF were measured by inductively coupled plasma atomic emission spectroscopy (ICP-AES, Jarrell-Ash ICAP9000, Franklin, MA, USA).

2.3 Osteoblast culture

Osteoblasts were isolated by sequential trypsin-collagenase-hyaluronidase digestion on the shank of 3-month old Sprague–Dawley rats supplied by animal center of West China Medical School, Sichuan University. In short, the shank was dissected and cut into small pieces under aseptic conditions and rinsed several times with phosphate-buffered saline (PBS) without calcium and magnesium. To minimize fibroblastic contamination and cell debris, the shank pieces

were incubated with 0.25% trypsin enzyme solution for 20 min, followed by five sequential digestions with 0.2% collagenase and 0.1% hyaluronidase in a metabolic shaker at 37°C for 1 h each. The supernatant of the first and second collagenase incubation, which contain high proportion of periosteal fibroblasts, were discarded. After continuous enzyme treatment, the supernatant was centrifuged (at 4000 r/min for 10 min) and the pellets were resuspended in RPMI-1640 culture medium supplemented with 10% fetal bovine serum (FBS) and maintained in a controlled humidified chamber at 37°C and 5% CO_2. Media were changed every 2 days until the cells reached confluence. Cells used for experiments were in the logarithmic phase of growth.

2.4 Effect of ionic products from three ceramic powder dissolutions on osteoblast proliferation

The method was carried out with dilutions of ceramic powder extracts in contact with osteoblasts. The dissolution extracts of three ceramics were prepared by adding their powders to RPMI 1640 culture medium according to International Standard Organization (ISO/EN 10993-5) [15]. The ratio of powder weight and the culture medium volume was 200 mg/ml. After incubation at 37°C for 24 h, the suspending liquid was centrifuged and the supernatant was collected. Subsequently, the diluted extracts (100, 25, 12.5 1.25 mg/ml) was prepared by adding FBS-free culture medium to the primary extract liquid for further experiments. The ion concentrations of the diluted extracts and RPMI 1640 culture medium were measured by ICP-AES.

The osteoblasts were plated into 96-well plates at a density of 5.0×10^3 cells/cm^2, and incubated for 6 h for cell adhesion. Then the culture medium was removed and replaced by 50 μl of RPMI-1640 medium containing 20% FBS and 50 μl of diluted extracts. The culture medium supplemented with 10% FBS without addition of diluted extracts was used as a control group. After being incubated at 37°C and 5% CO_2 for 1, 3, and 7 days, to detect the response of cells to material extracts, cell proliferation was evaluated by the quantitative 3-(4,5-dimethylthiazol-2-yl)-2,5-diphenyl tetrazolium bromide (MTT) assay, which based on the reduction of tetrazolium salt to formazan crystals by viable cells. In total, 100 μl of 5 mg/ml MTT solution was added in each well, followed by incubation for 4 h at 37°C. After incubation, 200 μl dimethyl sulfoxide (DMSO) was added in each well to stop the reaction between MTT and osteoblasts, and the samples were shaken until complete dissolution of the formed product had occurred. The optical density (OD) was measured at the wavelength of 590 nm using an enzyme-linked immunoadsorbent assay (ELISA) plate reader (EL × 800, BIO-TEK, Atlanta, GA, USA). And the OD value was direct proportional to the number of the living cells. The cell proliferation was determined with respect to the controls [25].

2.5 Osteoblast morphology and proliferation on the ceramic wafers

The osteoblasts were seeded on each opaque ceramic wafer at a density of 2.0×10^3 cells/cm^2 in a 24-well plate under the same culture conditions as described above. To evaluate osteoblast proliferation, the cells incubated in the culture medium without ceramics were used as a control group.

After culture for 3 and 7 days, the wafers were removed from the culture wells, rinsed with PBS and dehydrated in a graded ethanol series [30, 50, 70, 90, and 96% (v/v)] for 20 min, respectively, with final dehydration in absolute ethanol twice followed by critical point drying in liquid CO_2. Subsequently, the osteoblast morphology was observed by SEM.

Cell proliferation on three ceramic wafers was tested by the MTT assay. After the set culture time, MTT solution was added in each well, followed by incubation for 4 h at 37°C. Then DMSO was added to each well, and the samples were shaken until the formed formazan crystals were completely dissolved. Afterward, the 200 μl of solution of the said formed crystals in each well was transferred into a new 96-well plate for testing. The OD was measured at the wavelength of 570 nm by the ELISA plate reader.

2.6 Statistical analysis

The results are presented as Means ± SD ($n = 5$). Analysis of the results was carried out by using ANOVA and Bonferroni's post-test. A P value < 0.05 was considered statistically significant.

3 Results

3.1 Characterization of the three investigated single-phase ceramics

The XRD patterns of three investigated ceramics are shown in Fig. 1. Only the peaks of monticellite, akermanite and merwinite were detected. The full widths at half maximum (FWHM) of peaks were different among three XRD patterns. According to Scherer Formula and statistical theory, the average crystal sizes of monticellite, akermanite and merwinite ceramics were estimated from the FWHM and θ values as follows [26]: $\overline{\tau} = \frac{1}{n}\sum_{i=1}^{n} \tau_i = K\lambda/\beta_i \cos\theta_i$, where $\overline{\tau}$,τ_i, K, λ, β_i and θ_i are the average crystal size (which was the average of the sizes of crystals with different orientation indexes), the sizes of crystals with different orientation

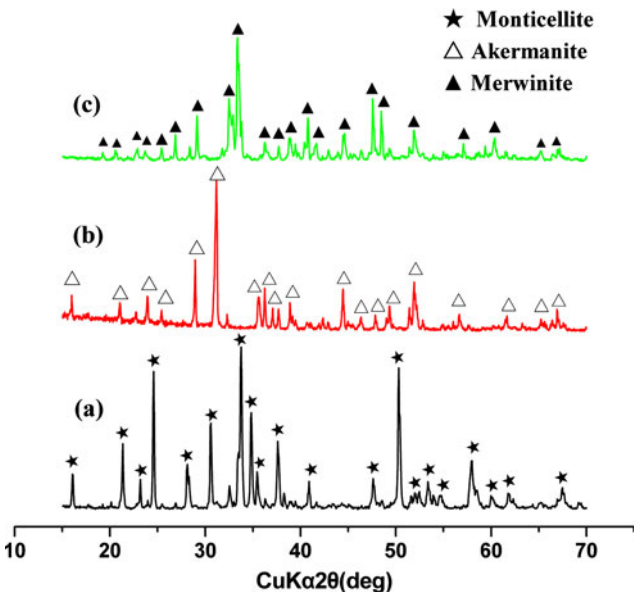

Fig. 1 XRD patterns of the three investigated single-phase ceramics. **a** monticellite, **b** akermanite, and **c** merwinite

indexes, the shape factor (typically 0.85–0.9), the X-ray wavelength (Å), the corrected FWHM (radians) of the diffraction peaks (which were the peaks marked in their XRD patterns, as shown in Fig. 1) used for determination of the sizes of crystals with different orientation indexes in ceramics, and the Bragg diffraction angle, respectively. The relative density, average crystalline sizes and mechanical properties of these ceramics are listed in Table 2. In total, the relative density and average crystal sizes of three bioceramics did not differ significantly from each other. Besides, the mechanical property of monticellite ceramics was the best, whereas that of merwinite ceramics was the worst.

3.2 Apatite-formation ability of three ceramics in SBF

Figure 2 shows the XRD patterns of monticellite, akermanite, and merwinite ceramics soaked in SBF for 14 days. It could be seen that the intensity of monticellte and akermanite peaks became lower (Fig. 2a, b), and the peaks of merwinite disappeared completely (Fig. 2c), while the characteristic peaks of bone-like apatite (JCPD 24-0033) appeared.

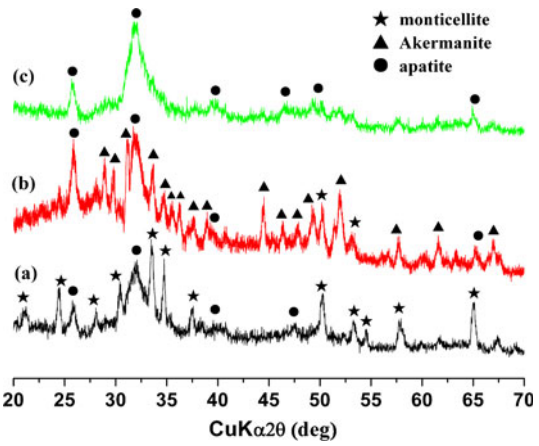

Fig. 2 XRD patterns of monticellite, akermanite, and merwinite ceramics soaked in SBF for 14 days. **a** monticellite, **b** akermanite, and **c** merwinite

The FTIR spectra of the surface products on the three SBF soaked ceramics are shown in Fig. 3. The bands existing in the broad ranges of 900–1500 and 400–600 cm^{-1} were the characteristic bands of bone-like apatite [9, 27, 28], and the broad bands from 900 to 1100 cm^{-1} were mainly attributed to the PO_4^{3-} absorption of the bone-like apatite [29]. The intensity of absorption peaks increased from monticellite to akermanite and merwinite ceramics with the decrease of MgO contents. These results were consistent with the results of the X-ray analysis of three ceramics soaked in SBF (Fig. 2).

The SEM micrographs of three ceramics soaked in SBF for 14 days are presented in Fig. 4, which show the different morphology of apatite formed on these ceramics. The apatite particles on monticellite ceramics were spherical and small, and the size was about 50–100 nm in diameter (Fig. 4a). The apatite on akermanite and merwinite ceramics presented worm-like morphology. The size of the apatite crystals on akermanite ceramics was about 100–300 nm in length and 50 nm in diameter (Fig. 4b), while that of the apatite crystals on merwinite ceramics was bigger and about 400–800 nm in length as well as 75 nm in diameter (Fig. 4c).

The P ion concentrations in SBF after soaking with three ceramics for 14 days are shown in Table 3. The concentration of P ions in freshly prepared SBF was 1.0 mM, and decreased to 0.33, 0.18, and 0.07 mM after soaking with monticellite, akermanite, and merwinite ceramics for

Table 2 The relative density, average crystalline sizes and mechanical properties of three ceramics

	Monticellite	Akermanite	Merwinite
Relative density (%)	92.7 ± 1.4	91.6 ± 3.2	91.3 ± 1.7
Average crystal sizes (Å)	605	611	555
Bending strength (MPa)	163.9 ± 3.6	141.8 ± 2.3	128.4 ± 4.7
Fracture toughness (MPa $m^{1/2}$)	1.65 ± 0.12	1.53 ± 0.10	1.57 ± 0.17
Young's modulus (GPa)	45.5 ± 4.1	56.2 ± 5.4	49.3 ± 2.3

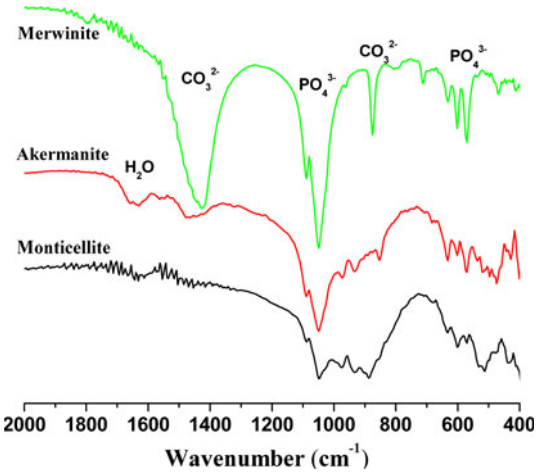

Fig. 3 FTIR spectra of the surface products of the three ceramics after being soaked in SBF for 14 days

14 days, respectively. The results revealed that the P ions in SBF were consumed during the formation of apatite on ceramics, and the rates of apatite formation on ceramics increased from monticellite to akermanite and merwinite ceramics. The merwinite ceramics with the lowest MgO content possessed the highest apatite-formation rate and ability.

3.3 Effect of ionic products from three ceramic powder dissolutions on osteoblast proliferation

Figure 5 shows the effect of extracts from ceramic powder dissolutions on osteoblast proliferation. The OD values of cells cultured with the diluted extracts whose concentrations were among 1.25 and 25 mg/ml were higher than the control, demonstrating that there was an obvious stimulatory effect on cell proliferation when the concentrations of the extracts were among 1.25 and 25 mg/ml. In addition, the stimulatory effect was most obvious at the concentration of 12.5 mg/ml for all the ceramics. When the extract concentration increased to 100 mg/ml, no obvious stimulatory effect on cell proliferation was detected and the merwinite extract even possessed an inhibitory effect on cell proliferation.

The corresponding concentrations of Ca, Mg, and Si ions in the three extracts and RPMI 1640 culture medium were shown in Table 4. It was clearly that the stimulatory effect on cell proliferation and concentrations of Ca and Mg ions were comparable among three ceramics when the extract concentration varied from 1.25 to 25 mg/ml. However, at the exact concentration of 1.25 mg/ml, the Si concentrations were almost zero and far lower than that of exact at 25 mg/ml. This result suggested that the difference of Si concentration has no obviously different effect on cell proliferation at this concentration range. At the concentration of 100 mg/ml, compared with those of the other two ceramic exacts, the Si concentration in merwinite exact was obviously higher and the Mg concentration was little lower, which might result in the inhibitory effect on cell proliferation. Furthermore, the combination of Ca, Mg, and Si ions in exact at the concentration of 12.5 mg/ml might be optimal for cell proliferation.

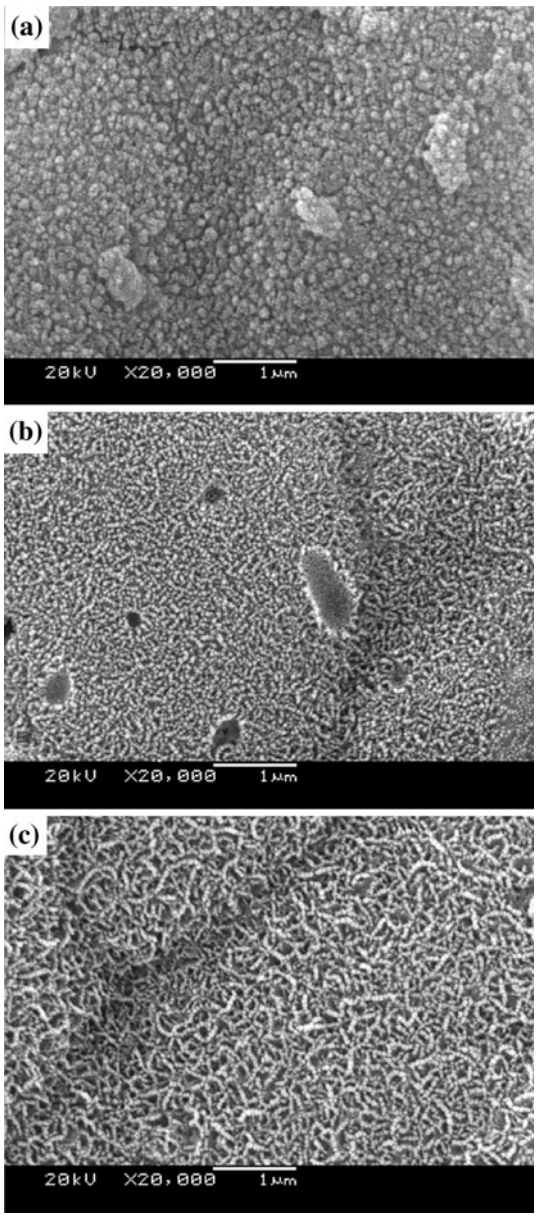

Fig. 4 SEM micrographs of the three ceramics soaked in SBF for 14 days. **a** monticellite, **b** akermanite, and **c** merwinite

Table 3 The P ion concentrations in SBF after soaking with three ceramics for 14 days

Solution	Freshly prepared SBF	Monticellite	Akermanite	Merwinite
P (mM)	1.0	0.33	0.18	0.07

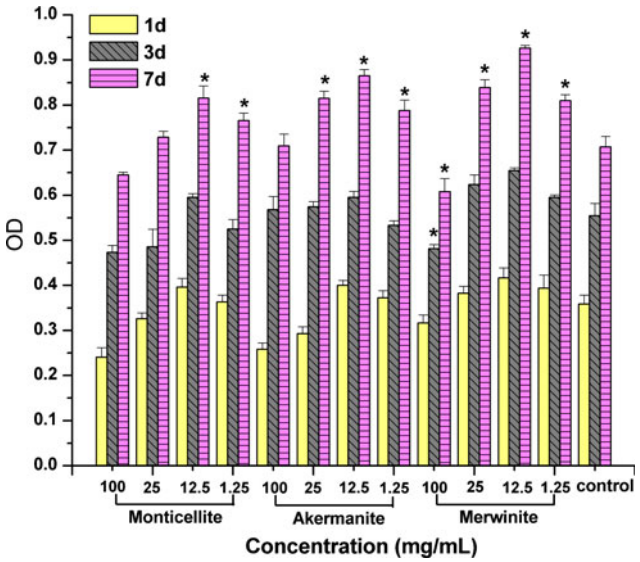

Fig. 5 Effect of extract from ceramic powder dissolution on osteoblast proliferation, OD on y-axis is direct proportional to the number of the living osteoblasts

3.4 Osteoblast morphology and proliferation on the ceramics

The SEM micrographs show the morphological features of osteoblasts cultured on the ceramic wafers for 7 days (Fig. 6). It was obvious that cells attached on the three ceramics and presented a close contact with ceramic surfaces after culture. The osteoblasts on monticellite ceramics were flattened and elongated (Fig. 6a). The cells on akermanite and merwinite ceramics formed a confluent layer and showed a spread appearance; moreover, the filopodias were apparent (Fig. 6b, c). The mentioned morphological features of osteoblasts on merwinite ceramic were more obvious than the other two ceramics (Fig. 6c).

Figure 7 displays the results of osteoblast proliferation on three ceramic wafers after culture for 3 and 7 days. It clearly showed that cells on them proliferated with the increase of the culture time. In total, after being incubated for 3 and 7 days, the OD values of osteoblasts on the ceramics were significantly higher compared with the control. In the first 3 days, there were no evident differences in the proliferation levels of cells on three ceramics. After 7 days of incubation, the OD values all became higher, and the proliferation of osteoblasts was more obvious. Cells on monticellite ceramics showed the lowest proliferation level, and the cells on merwinite ceramics presented a little higher proliferation level than that of cells on akermanite ceramics.

4 Discussion

The results of this research showed that the mechanical properties of three ceramics were improved from merwinite to akermanite and monticellite ceramics. According to previous studies, the chemical composition, relative density, and average crystal size are very important factors affecting the mechanical properties of ceramics [16, 30, 31]. Our results suggested that the relative density and average crystal sizes of the three bioceramics did not differ significantly from each other, so the different mechanical properties of three ceramics could be due to the difference in chemical composition of starting materials. As shown in Table 2, according to the order of monticellite, akermanite, and merwinite ceramics, with the decrease of MgO content, the mechanical strengths of ceramics decreased. It was indicated that Mg played an important role in affecting the mechanical properties of bioactive ceramics in the MgO–CaO–SiO_2 system, and the mechanical properties of ceramics in this system might be controlled by adjusting the MgO contents.

Some documents also reported that bond energy of Mg–O was higher than that of Ca–O bond [32]. In this study, all the

Table 4 The Ca, Si, and Mg ion concentrations in the extracts of ceramic powders and RPMI 1640 culture medium (mM)

Ion concentrations	Extract concentrations (mg/ml)				Ceramics and culture medium
	100	25	12.5	1.25	
Ca	0.93	0.56	0.51	0.44	Monticellite
	1.07	0.60	0.53	0.45	Akermanite
	1.14	0.63	0.54	0.45	Merwinite
	0.42				Culture medium
Mg	2.83	0.94	0.62	0.33	Monticellite
	2.61	0.88	0.59	0.32	Akermanite
	2.27	0.79	0.55	0.32	Merwinite
	0.31				Culture medium
Si	1.49	0.35	0.19	0.02	Monticellite
	1.75	0.44	0.23	0.02	Akermanite
	2.78	0.70	0.37	0.04	Merwinite
	0				Culture medium

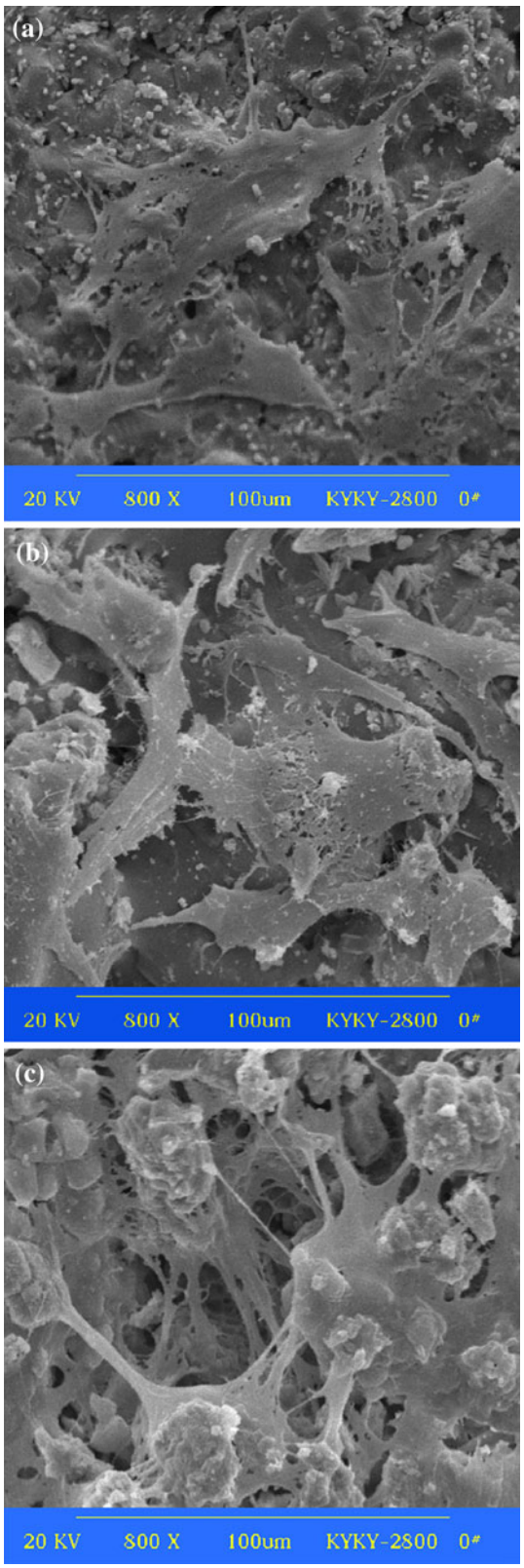

Fig. 6 SEM micrographs of cells cultured on the three ceramic wafers for 7 days. **a** monticellite, **b** akermanite, and **c** merwinite

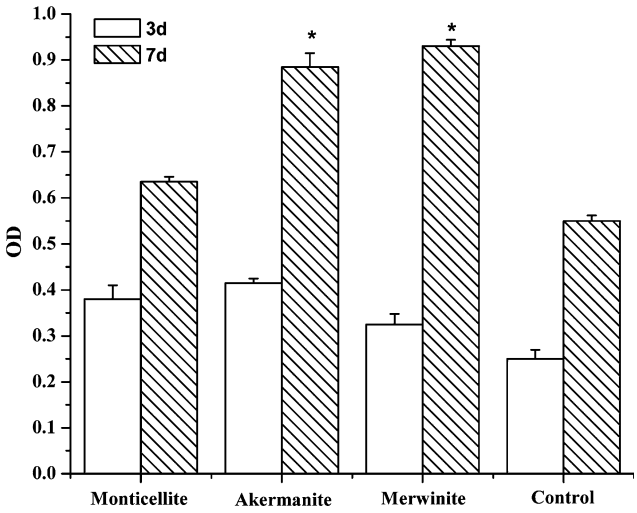

Fig. 7 Osteoblast proliferation on three ceramics after culture for 3 and 7 days. OD on y-axis is direct proportional to the number of the living osteoblasts

three ceramics are Mg-containing $CaO–SiO_2$ based materials. With the increase of MgO contents, Mg atoms might occupy the position of Ca atoms and make the crystal structure more stable, thus the ceramics with higher-MgO content displayed higher mechanical strength. Besides, crystal structure might also affect the mechanical properties of the ceramics [33, 34]. It is known that the crystal structures of the three ceramics are different. Monticellite is trimetric, akermanite is tetragonal, and merwinite is monoclinic. The differences in crystal structures might result in the differences among the mechanical properties of the ceramics. However, further studies are required to determine the relationship between the crystal structures and the mechanical properties of the ceramics.

Previous studies showed bone-like apatite played an essential role in the formation, growth and maintenance of the tissue-biomaterial interface, and this bone-like apatite layer could be reproduced in SBF [17]. Our results indicated that monticellite, akermanite, and merwinite ceramics possessed different apatite-formation ability in SBF. In this research, the increase trend of the apatite peak intensity and particle size as well as the decrease of P ion concentration in SBF suggested that the apatite-formation ability of ceramics increased from monticellite to akermanite and merwinite ceramics with the decrease of MgO content, which revealed that MgO possessed an inhibiting effect on the apatite formation ability of the ceramics in the $MgO–CaO–SiO_2$ system.

Ducheyne et al. [35] found that apatite-formation ability was directly relative to the dissolution of the materials. According to the mechanisms of nucleation and growth of apatite on the ceramics proposed by Hench, the rate of

apatite formation increased with the increase of bioglass dissolution [4]. In the present study, three kinds of ceramics are all Mg-containing $CaO–SiO_2$ based materials. As the above-mentioned, Mg–O bond energy was higher than that of Ca–O bond, and the higher Mg–O bond energy made it difficult to release atoms from crystal lattice compared with Ca–O bond [32]. Hence, with the increase of MgO contents, the dissolution rate decreased with the increase of the stronger Mg–O bonds from merwinite to akermanite and monticellite ceramics, resulting in the slower Ca ion release and decrease of apatite-formation ability of ceramics.

Previous studies disclosed that bioactive glass–ceramics in $MgO–CaO–SiO_2$ system could release Ca, Mg and Si ions/groups thereof [15, 17, 18]. Recently, some document reported that Si containing ion products could promote cell proliferation and gene expression [36, 37]. In the present study, the MTT tests suggested that the Ca, Si, and Mg containing ionic products from the dissolutions of merwinite, akermanite and monticellite ceramics at certain concentration could also stimulated cell proliferation markedly, and the combination of Ca, Mg, and Si ions at this concentration might be optimal for cell proliferation, which was in accordance with the previous results [36–38]. Furthermore, it was obvious that the Si concentrations in the extracts of three ceramics were much higher than those in cell culture medium (no Si ions/groups in the controls), indicating that Si ions at low concentration might be one of important factor for the stimulatory effect on osteoblast proliferation. However, at high concentration of extracts, the inhibitory effect of merwinite exact on cell proliferation was more obvious than the other ceramics. The corresponding Si concentration from merwinite was markedly higher and Mg concentration was lower when compared with the other ceramics, which suggested that higher Si concentration and lower Mg concentration might be responsible for the inhibitory effect on cell proliferation.

The SEM micrographs showed that cells could attach and spread well on all the ceramics and present a close contact with ceramic surfaces after culture. The cells on merwinite ceramics displayed the most obvious morphological features, while there was no significant morphological difference between cells on akermanite and monticellite ceramics, which was similar to the results of cell proliferation on ceramic wafers. In this study, the differences in the morphological features and proliferation of osteoblasts on these ceramics might result from the ionic products from three ceramics with different MgO contents and solubility.

5 Conclusion

In conclusion, three bioceramics in the $MgO–CaO–SiO_2$ system were prepared firstly, and then their mechanical properties, bioactivity and cytocompatibility were evaluated and compared. The mechanical properties were improved from merwinite to akermanite and monticellite ceramics with the increase of MgO contents, and the apatite-formation ability in SBF as well as the cell proliferation decreased. The Ca, Mg and Si-containing ionic products at certain concentration could significantly stimulated cell proliferation. Osteoblasts could adhere, spread and proliferate on these ceramic wafers. In addition, the morphological features and proliferation of cells on merwinite ceramics were more obvious than those of cells on the other two ceramics. Our results indicated that the MgO content was one of the important factors, which distinctly affected the mechanical properties and biological performances of bioceramics in the $MgO–CaO–SiO_2$ system. The difference of Si concentration possessed no obvious effect on cell proliferation at certain concentration range, and higher Si concentration and lower Mg concentration might inhibit cell proliferation. Furthermore, the combination of Ca, Mg, and Si ions in merwinite exact at the concentration of 12.5 mg/ml might be optimal for cell proliferation, which could be consulted when designing the chemical compositions of materials in the $MgO–CaO–SiO_2$ system.

Acknowledgments Financial supports from the Fund for Excellent Young Researchers of the Sichuan Province, China (07ZQ026-118) are gratefully acknowledged.

References

1. Hench LL, Splinter RJ, Allen WC, Greenlee TK. Bonding mechanism at the interface of ceramic prosthetic materials. J Biomed Mater Res. 1972;2:117–41.
2. Kokubo T, Ito S, Sakka S, Yamamuro T. Formation of a high-strength bioactive glass-ceramic in the system $MgO–CaO–SiO_2–P_2O_5$. J Mater Sci. 1986;21:536–40.
3. Ohura K, Nakamura T, Yamamuro T, Kokubo T, Ebisawa T, Kotoura T. Bone-bonding ability of P_2O_5 free $CaO{\cdot}SiO_2$ glasses. J Biomed Mater Res. 1991;25:357–65.
4. Hench LL. Bioceramics. J Am Ceram Soc. 1998;81:1705–28.
5. Wilson J, Yli-Urpo A, Happonen RP. Bioactive glasses: clinical application. In: Hench LL, Wilson J, editors. An introduction to bioceramics. Advances series in ceramics. Singapore: World Scientific Publishing; 1993. p. 63–74.
6. Oliveira JM, Correia RN, Fernandes MH. Surface modifications of a glass and a glass-ceramic of the $MgO–3CaO{\cdot}P_2O_5–SiO_2$ system in a simulated body fluid. Biomaterials. 1995;16:849–54.
7. Merrollli A, Tranquilli Leali P, Guidi PL. Comparison in vivo response between a bioactive glass and non-bioactive glass. J Mater Sci: Mater Med. 2000;11:219–22.
8. Siriphannon P, Hayashi S, Yasumori A, Okada K. Preparation and sintering of $CaSiO_3$ from coprecipitated powder using NaOH as precipitant and its apatite formation in simulated body fluid solution. J Mater Res. 1999;14:529–36.
9. Siriphannon P, Kameshima Y, Yasumori A, Okadaa K, Hayashi S. Formation of hydroxyapatite on $CaSiO_3$ powders in simulated body fluid. J Eur Ceram Soc. 2002;22:511–20.

10. Lin KL, Zhai WY, Chang J, Zeng Y, Qian WJ. Study of mechanical property and in vitro biocompatibility of $CaSiO_3$ ceramics. Ceram Inter. 2005;31:323–6.
11. Nakajima S, Kurihara Y, Wakatsuki Y, Noma H. Physicochemical characteristics of new reinforcement ceramic implant. Shikwa Gakuho. 1989;89:1709–17.
12. Nakajima S. Experimental studies of healing process on reinforcement ceramic implantation in rabbit mandible. Shikwa Gakuho. 1990;90:525–53.
13. De Aza PN, Luklinska ZB, Anseau M. Bioactivity of diopside ceramic in human parotid saliva. J Biomed Mater Res B Appl Biomater. 2005;73B:54–60.
14. Nonami T, Tsutsumi S. Study of diopside ceramics for biomaterials. J Mater Sci: Mater M. 1999;10:475–9.
15. Wu CT, Chang J, Ni SY, Wang JY. In vitro bioactivity of akermanite ceramics. J Biomed Mater Res A. 2006;76:73–80.
16. Wu CT, Chang J. A novel akermanite bioceramic: preparation and characteristics. J Biomater Appl. 2006;21:119–29.
17. Wu CT, Chang J, Wang JY, Ni SY, Zhai WY. Preparation and characteristics of a calcium magnesium silicate (bredigite) bioactive ceramics. Biomaterials. 2005;26:2925–31.
18. Chen XC, Ou J, Kang YQ, Huang ZB, Zhu HY, Yin GF, et al. Synthesis and characteristics of monticellite bioactive ceramic. J Mater Sci: Mater Med. 2008;19:1257–63.
19. Ou J, Kang YQ, Huang ZB, Chen XC, Wu J, Xiao RC, et al. Preparation and in vitro bioactivity of novel merwinite ceramic. Biomed Mater. 2008;3:1–8.
20. Kanzaki N, Onuma K, Treboux G, Tsutsumi S, Ito A. Inhibitory effect of magnesium and zinc on crystallization kinetics of hydroxyapatite (0001) face. J Phys Chem B. 2000;104:4189–94.
21. Webster TJ, Ergun C, Doremus RH, Bizios R. Hydroxyapatite with substituted magnesium, zinc, cadmium, and yttrium II: mechanisms of osteoblast adhesion. J Biomed Mater Res. 2002; 59:312–7.
22. Liu CC, Yeh JK, Aloia JF. Magnesium directly stimulates osteoblast proliferation. J Bone Miner Res. 1988;3:S104.
23. Ni SY, Chang J, Chou L. In vitro studies of novel $CaO–SiO_2–MgO$ system composite bioceramics. J Mater Sci: Mater Med. 2008;19:359–67.
24. Kokubo T, Takadama H. How useful is SBF in predicting in vivo bone bioactivity? Biomaterials. 2006;27(15):2907–15.
25. Macaroff PP, Oliveira DM, Ribeiro KF, Lacava ZGM, Lima ECD, Morais PC, et al. Studies of cell toxicity of complexes of magnetic fluids and biological macromolecules. J Magn Magn Mater. 2005;293:293–7.
26. Chen JJ, Gao Y, Zeng F, Li DM, Pan F. Effect of sputtering oxygen partial pressures on structure and physical properties of high resistivity ZnO films. Appl Surf Sci. 2004;223:318–29.
27. Sivakumar M, Rao KP. Preparation, characterization and in vitro release of gentamicin from coralline hydroxyapatite-gelatin composite microspheres. Biomaterials. 2002;23:3175–81.
28. Zeng HT, Lacefield WR. XPS, EDX and FTIR analysis of pulsed laser deposited calcium phosphate bioceramic coatings: the effects of various process parameters. Biomaterials. 2000;21:23–30.
29. Weng J, Liu Q, Wolke JGC, Zhang XD, De GK. Formation and characteristics of the apatite layer on plasma-sprayed hydroxyapatite coatings in simulated body fluid. Biomaterials. 1997;18: 1027–35.
30. Lin KL, Chang J, Lu JX, Wu W, Zeng Y. Properties of β-$Ca_3(PO_4)_2$ bioceramics prepared using nano-size powders. Ceram Inter. 2007;33:979–85.
31. Ni SY, Chou L, Chang J. Preparation and characterization of forsterite (Mg_2SiO_4) bioceramics. Ceram Inter. 2007;33:83–8.
32. Vallet-Regí V, Salinas AJ, Roman J, Gil M. Effect of magnesium content on the in vitro bioactivity of $CaO–MgO–SiO_2–P_2O_5$ sol–gel glasses. J Mater Chem. 1999;9:515–8.
33. Gassan J, Bledzki AK. Alkali treatment of jute fibers: relationship between structure and mechanical properties. J Appl Polym Sci. 1999;71:623–9.
34. Ziegler G, Heinrich J, Wötting G. Review relationships between processing, microstructure and properties of dense and reaction-bonded silicon nitride. J Mater Sci. 1987;22:3041–86.
35. Ducheyne P, Radin S, King L. The effect of calcium phosphate ceramic composition and structure on in vitro behavior. I. Dissolution. J Biomed Mater Res. 1993;27:25–34.
36. Xynos ID, Edgar AJ, Buttery LD, Hench LL, Polak JM. Gene expression profiling of human osteoblasts following treatment with ionic products of bioglass 45S5 dissolution. J Biomed Mater Res. 2001;55:151–7.
37. Valerio P, Pereira MM, Goes AM, Leite MF. The effect of ionic products from bioactive glass dissolution on osteoblast proliferation and collagen production. Biomaterials. 2004;25:2941–8.
38. Gough JE, Notingher I, Hench LL. Osteoblast attachment and mineralized nodule formation on rough and smooth 45S5 bioactive glass monoliths. J Biomed Mater Res. 2004;68:640–50.